[1]Laila Osama
[2]Asmaa Salah,
[2]Saber M. Saleh
[3] Mohamed Kourany

Meta-heuristic Optimization for Wind Turbine Control: Evaluating Performance with PI and Fractional PI Controllers for Maximum Power Extraction

Journal of Electrical Systems

Abstract: **-** Here, MATLAB Simulink is used to model wind energy systems. Because of the wind turbine's nonlinear characteristics, the model tracks the highest possible output extracted from wind energy using the maximum power point tracking (MPPT) technique. The model includes a grid-connected wind energy conversion system (WECS) with a back-to-back power converter, a direct-driven permanent magnet synchronous generator (PMSG), and an MPPT controller. Control architectures based on field and voltage-oriented control techniques are recommended for machine- and grid-side converters. The terms "Artificial Rabbit Optimizer, "Red-Tailed Hawk Optimizer," and "Grey Wolf Optimizer " refer to optimization techniques that yield analytical formulations for choosing the parameters of the proportional-integral (PI) controllers and fractional PI controller engaged in various control loops. Result By utilizing specific PI controller parameters the wind gust perturbation is used to compare the MPPT's controller PI traditional and PI^α fractional. The transient system simulation is constructed via MATLAB to assess the efficacy of the PMSG-based WECS in fluctuating wind conditions. This paper explores how the control methods result in high performance, minimum torque fluctuations, and minimum transient and steady-state errors.

Keywords: Artificial rabbit optimizer, Red-tailed hawk optimizer, grey wolf optimizer, (WECS), (MPPT), (PMSG).

I. INTRODUCTION

Now, applications of (PMSGs) in (WECS) have increased dramatically. The purpose of the wind turbine is to transform wind energy into mechanical rotational energy. The installed wind turbine and generator cause's overall average power rating has increased significantly. In low-speed direct-driven wind turbine systems, multipole PMSG is a valuable technology that can reduce the high maintenance costs of gearboxes. Reliability is raised and expenses are reduced when wind turbine systems without a gearbox are used. Power conversion devices must be used to convert the electrical energy generated by the PMSG generator. The converter systems allow the generator's speed and electromagnetic torque to be controlled and the ability to alter the power flow to the AC grid; a wide variety of (WECS) is produced by varying the designs and configurations of power converters. The properties of the (WECS) can be improved by applying A system with a full-ability power converter [1-5].

The model system and control methodologies include a grid-side inverter, a generator-side inverter, and a PMSG wind turbine model. The generator-side inverter and grid-side inverter controller employ back-to-back space vector pulse width modulation (SVPWM) to decouple the management of the active and reactive power [6-7]. The (MPPT) modifies the rotating speed to get the maximum power from the wind. A control method founded on the vector control technique has been investigated to create converters. As the generator's output potential and frequency fluctuate with variations in wind velocity, the side rectifiers monitor the

[1]Laila Osama Faculty of Engineering, Fayoum University, Fayoum, the Electrical Power and Renewable Energy Department, Faculty of Engineering, Nahda University in Beni Suef, Egypt. (e-mail: laila.osama@nub.edu.eg).
[2] Asmaa Salah is with the Electrical Power and Machine Department, Faculty of Engineering, Fayoum University, Fayoum, Egypt (asf00@fayoum.edu.eg).
[2]*Corresponding author: Saber M. Saleh is with the Electrical Power and Machine Department, Faculty of Engineering, Fayoum University, Fayoum, Egypt (sms08@fayoum.edu.eg).
[3] Mohamed Saad is with the Electrical Power and Renewable Energy Department, Nahda University in Beni Suef, Egypt. (e-mail: mohammed.saad@nub.edu.eg).

maximum wind power. Plus, the inverter regulates the grid-side power factor and maintains the DC-bus voltage.

Additionally, the active and reactive powers are controlled by the grid-side inverter, respectively. The DC link makes decoupling between the generator-side converters and the grid-side inverter feasible [8–10]. The PI control rule and the most effective way to deal with control issues form the basis of most industrial controllers still in use today. Most industrial controllers nowadays depend on the PI control rule, which offers the most simple, practical, and efficient answer to control issues. To achieve the intended control responses during control system commissioning, parametric tuning and optimization of the PI controller are the majority of critical engineering tasks. The PI controller's parametric tuning balances robustness to withstand large-signal disturbances and stability and quickness of reaction to small-signal disturbances [11-13]. Response-surface method (RSM), artificial neural network (ANN), Taguchi technique, Grey Wolf Optimizer (GWO) [11,12], Artificial Rabbit Optimizer (ARO) [13], and Red Tiled Hawk algorithm [14] are several examples of statistical and conventional techniques used to fine-tune the gain factors of PI regulators used in many power system applications. However, these methods depend on the initial values [14-16].

Applying Meta-Heuristic Optimization to Wind Turbine Control Meta-heuristic optimization techniques have successfully optimized PI and FPI controller parameters for wind turbine control. Key research areas include:

(MPPT):

- Enhancing controller parameters to track the (MPP) of the (WT).
- Grid Integration: Ensuring stable and efficient integration of the (WT) into the electrical grid.
- Load Reduction: Minimizing mechanical strain on the turbine's constituent parts.
- Fault Detection and Diagnosis: Using optimization methods to create algorithms for wind turbine system problem diagnostics and early detection.[17]

In reference [11], This study looks at a model of a variable-speed wind turbine with a 2 MW PMSG added. This study does not focus on the converter (grid and rotor sides) or its controls, REF. [14]. This study presents wind energy system modeling using MATLAB Simulink. The model is considered the (MPPT) technique to monitor the most amazing power generated from wind energy because wind turbines are nonlinear. The model includes a wind-generating model, a DC-DC converter, and an MPPT controller. Their main contribution is creating a comprehensive model of a DC-DC converter, also known as a buck converter. It enables the MPPT controller's duty cycle to modify the converter's input voltage to follow the wind generator's greatest output points. REF. [18] This research analysed the performance of multiple MPPT algorithms based on their different speed responses and capacity to obtain the best energy yield. Because of its simplicity, based on simulation data available in the literature, the most effective MPPT technique for wind energy systems is the optimal torque control (OTC) approach. However, despite its flexibility and ease of use, Finding the best course of action requires assistance because the perturbation and observation (P&O) method isn't effective. REF. [2] Modelling a PMSG that generates power for the utility grid using a remote-controlled wind turbine is the aim of our paper, the efficacy of the PMSG wind power plant, which is used by remote controllers, is sw demonstrated. For highly autonomous operationWind turbines connected to the grid are controlled by two inverters with a voltage supply. When necessary, the generator-side inverter disconnects the syn. Generator from the grid and regulates it. The grid-side inverter controls the power transfer between the direct current (DC) bus and the AC side. They are both set up to be managed by a back-to-back frequency converter that uses SVPWM. Additionally, inverters are controlled using an improved proportional-integral (PI) controller. REF. [6] A grid-connected system (WECS) that uses a back-to-back power converter and a direct-driven miniature (PMSG) is illustrated in their study. Control architectures based on field and voltage-oriented control techniques are recommended for machine- and grid-side converters. In a variety of control loops, the words "modulus optimum" and "symmetric optimum" describe optimization methods that produce analytical formulas for choosing the parameters of the (PI) controllers.

REF. [17]. The use of meta-heuristic optimization, more especially particle swarm optimization, in the design of fractional order PI (FPI) controllers for wind turbines (MPPT), is thoroughly examined in this research. It makes a significant addition to the field by Comparing (PI^{α}) controllers with traditional PI controllers. The paper demonstrates the superior performance of (PI^{α}) controllers in quick response time and reduced steady-state error.

- Using PSO for optimization: PSO is a primitive meta-heuristic algorithm that effectively tunes controller parameters.
- Considering wind speed variations: In this research, the use of the improved controllers under various wind speed situations is evaluated.
- By studying this paper, anyone can gain insights into the application of meta-heuristic optimization for wind turbine control, the benefits of using (PI^{α}) controllers, and the potential improvements in power extraction that can be achieved through optimal controller design.

In REF. [19] A meta-heuristic optimization is presented here -based (MPPT) control for a (WECS) with a (PMSG). The approach uses a (PSO algorithm for the controller's optimization parameters of a (PI^{α}) controller.

REF. [20] This work provides a hybrid optimization strategy for wind turbine control that combines (PSO) and genetic algorithms (GA). The proposed approach is used to optimize the parameters of a PI controller for maximum power extraction.

REF. [21] This project aims to optimize and control a renewable energy system consisting of (PMSG) connected to a direct-drive Horizontal-Darrieus wind turbine (DDH-DWT). The aim is to apply cutting-edge optimization techniques to maximize wind energy extraction. The control issue is an optimization problem, with the difficulty of determining the optimal controller parameters.

REF. [22] The best control method can significantly increase the variable speed (WECS's) effectiveness. A wind turbine with variable speed is used in the wind energy converter system described in the research. It includes control circuits, a grid-side converter, a machine-side converter, and a wind turbine with a (PMSG).

The PMSG generator and the wind power system mathematical model have been explained. The vector control methods-based converter system control algorithms have been implemented. The optimal control method has been applied in the machine-side converter's control system.

REF. [23] This research uses MATLAB Simulink to model and simulate (WECS) based on PMSG. The (WT), PMSG, diode rectifier, DC-DC converter (Buck-Boost), and SVPWM-based inverter are all included in this model. The output voltage fluctuates constantly because of wind fluctuations. The DC voltage can be kept constant by controlling the Cuk Converter. For stand-alone loads (remote places, islands, hill stations, etc.), an SVPWM-based inverter can generate a steady output voltage and frequency. The developed model is consistent with the theoretical estimations.

REF [24]. To control the frequency and magnitude of the load voltage in different operational circumstances

, this study discusses the control strategy of a freestanding wind-powered Permanent Magnet Synchronous Generator (PMSG). The performance characteristics of the wind-generating system under three distinct operating conditions wind-speed variation, load variation, and unbalanced operating condition have been thoroughly examined.

Verified that the control method effectively maintained a consistent load voltage and frequency under various operational conditions. To obtain the DC-link voltage at a predetermined level, the duty cycle of the utilized DC-DC boost converter has been controlled. The usefulness of the control approach in preserving a steady load voltage and frequency under varied operating conditions was confirmed by the simulation results. This has been accomplished by regulating the DC-DC boost converter's duty cycle to keep the DC-link voltage constant at a preset value. In REF. [25] a new WECS control based on grid-connected PMSG has been introduced. Control algorithms based on the sliding mode (SM) method have been researched for

the system. Additionally, the concept of MPPT has been described in terms of how the pitch angle strategy controls wind speed and how the PMSG rotor speed is modified based on the current wind speed.

There are two control strategies in place for both grid-side and generator-side converters. Utilizing SM nonlinear control, which adjusts the generator's rotational speed in response to variations in wind speed, speed control is achieved. Furthermore, the inverter is managed to preserve and control the DC-bus voltage and grid power factor by the use of the SM technique. An SM nonlinear control is utilized to achieve speed control, whereby the generator's rotational speed is adjusted based on variations in wind speed via the q-axis current. Furthermore, employing the SM technique, the grid power factor and DC-bus voltage are maintained and regulated by controlling the inverter, the WECS and PMSG together can harness the maximum wind power and sustain the output voltage's frequency and amplitude while maintaining a unity power factor and little distortion. Ultimately, the simulation results demonstrate that the proposed nonlinear SM controllers are very efficient for the WECS and confirm that the suggested control architecture is applicable and effective.

REF. [26] This paper produces the democratic joint operations algorithm (DJOA), a novel meta-heuristic algorithm inspired by military philosophy. To deliver MPPT under different wind speed profiles, its target is to determine the best proportional-integral-derivative (PID) controller parameters for the WECS based on a PMSG.

To do a more in-depth optimal search.in REF. [27] This study proposed an optimally adjusted PI control system for grid-connected WECS-based PMSG. The PMSG and grid are directly interfaced via a current-controlled matrix converter. The PMSG speed is maintained at the reference speed that maximizes wind energy extraction by adjusting the PI controller parameters using the enhanced BFO algorithm. One objective function that has been evaluated because of its benefits is the integral time absolute error (ITAE) performance index, above alternative performance metrics. Additionally, by limiting the reactive power delivered to the system during disturbances through grid code constraints, the proposed control system includes LVRT capabilities. PSCAD/EMTDC, connected to MATLAB software, simulates the suggested system to show its efficiency and quick responsiveness under various operating circumstances. It has been taught that the recommended control strategy, which controls the generator's d-axis current for getting the greatest active power under standard wind speeds, has a quick dynamic reaction. Additionally, the simulation findings show that the control system is valuable and can respond quickly to a grid failure.

- This work aims to investigate MPPT algorithms for (WECS) that use back-to-back converters that are powered by PMSG and tied to the grid.
- This paper aims to study the control methods mentioned above.

This paper is arranged as follows: In Sections 2 and 3, the (WT) generator and the multipole PMSG models are demonstrated. In Section 3, the nonlinear control of WECS is presented. Section 4 contains the results.

II. METHODS

As illustrated in Figure 1, the proposed WECS's main components are a wind turbine, a PMSG with surface-mounted permanent magnets, a frequency converter made up of two current-regulated PWM VSCs, a grid-side converter (GSC) and a machine-side converter (MSC), and a standard DC-link capacitor in between.

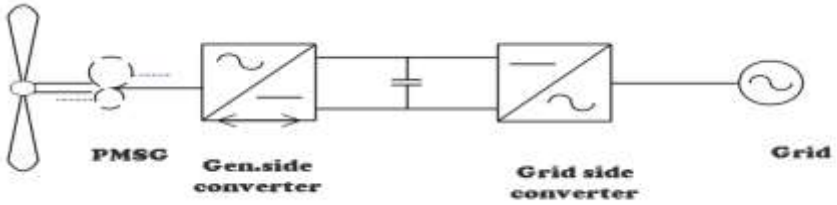

Fig 1. WECS

A. Wind turbine model

The output power of the (WT) is shown here.

$$P_m = 0.5\rho A {v_\omega}^3 C_P \quad (1)$$

P_m, ρ, C_P, A, r, and $v_\omega$are, respectively, wind speed, air density, power coefficient, swept area ($A = \pi r^2$), turbine blade radius, and turbine output power. The pitch angle β and tip-speed ratio λ determine the power coefficient which is written as

$$C_P(\lambda, \beta) = c_1 \left(\frac{c_2}{\lambda_i} - c_3\beta - c_4\right) e^{-c5/\lambda_i} + c_6\lambda \quad (2)$$

$$\frac{1}{\lambda_i} = \frac{1}{\lambda + 0.08\beta} - \frac{0.035}{\beta^3 + 1} \quad (3)$$

The coefficients c_1- c_6 for different (WT) may differ because this function is related to the kind of rotor used in (WT). The suggested coefficients are: c_1 = 0.5176, c_2= 116, c_3= 0.4; c_4 = 5, c_5= 21, and c_6 = 0.0068. Additionally, β which is the angle formed by the blade's cross-section chord and the plane of rotation, and the tip-speed ratio is

$$\lambda = \frac{r\omega_m}{v_w} \quad (4)$$

ω_m is the angular speed of the WT (rad/s) [18].

B. Generator model

In the d-q reference frame, the PMSG equations are written as

$$\frac{di_{sd}}{dt} = -\frac{R_s}{L_{sd}} i_{sd} + \omega_e \frac{L_{sq}}{L_{sd}} . i_{sq} + \frac{1}{L_{sd}} V_{sd} \quad (5)$$

$$\frac{di_{sq}}{dt} = -\frac{R_s}{L_{sq}} i_{sq} - \omega_e \left(\frac{L_{sd}}{L_{sq}} . i_{sd} + \frac{1}{L_{sq}} \psi_p\right) \frac{1}{L_{sq}} Vsq \quad (6)$$

The electromagnetic torque in the rotor can be shown as follows

$$T_e = \frac{1.5P}{2} [\, \Psi_p \, i_{sq} + i_{sq} i_{sd} (L_{sd} - L_{sq})] \quad (7)$$

There, isd, isq, Vsd, and Vsq Are the q-axis and d-axis currents and voltages the corresponding stator resistance ωe is the fundamental electrical angular frequency of the generator. Symbolize the inductance of the generator. Figure 4 shows the PMSG's comparable circuit on the dq-rotating reference frame. Permanent flux is represented by ψp, stator resistance by Rs, and the number of poles by P [26].

The Equation of the drive train of the (WT) system is given as

$$\frac{d\omega_m}{dt} = \frac{1}{J}(T_w - T_e - B\omega_m) \quad (8)$$

where J represents the turbine and generator's combined inertia, B represents the rotational damping, θ represents the generator's mechanical angle, and T_w represents the aerodynamic torque delivered to the generator side by

$$T_{w-g} = T_w / n_g, \; n_g \text{ is the gear ratio, } n_g = 1.$$

C. MPPT profile

To optimize wind power, it is necessary to obtain the Cp (λ, β) at its highest point C_{P*} at different wind velocities within the operating range. Specifically, the β is held at a value that gives the maximum C_{P*}, while the tip-speed-ratio λ is maintained at its optimum value λ∗.

$$C_{P*} = C_P(\lambda^*)$$

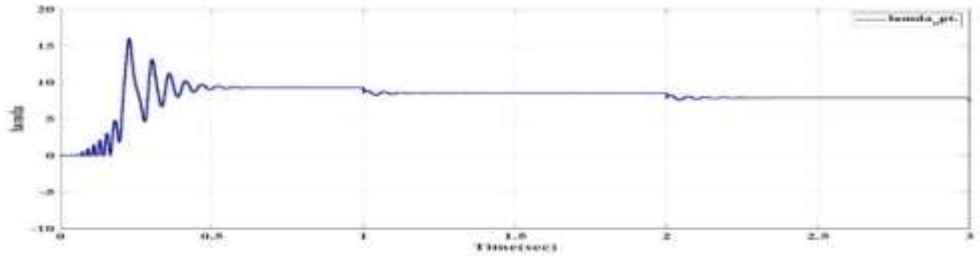

Fig 2. lamda optimuim

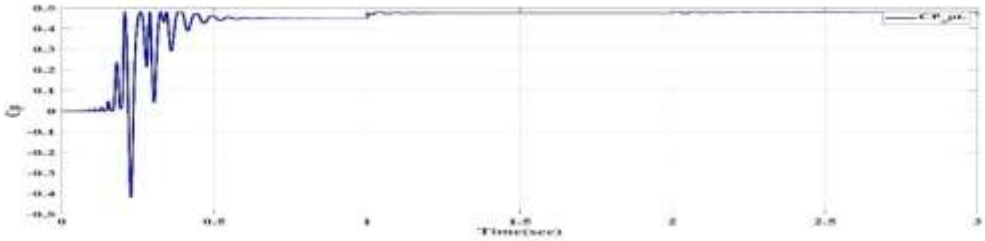

Fig 3. Optimum power coefficient

It, therefore, needs ω_m to follow its ideal reference. ω_{m*} as follows

$$\omega_{m*} = \frac{v_w}{r}\lambda^* \quad (9)$$

Here, the β = 0°, the optimal λ^*= 8.5 while C_P = 0.45 [10]. Fig. 2&3 show the C_P and λ waveforms. These waveforms show how the MPPT algorithm keeps the C_P and λ values at their reference and maximum values.

D. Generator side converter control scheme

Maximizing power output from the input source is MSC's main goal. Two control loops make up MSC's field-oriented control structure: the outer PMSG speed control loop and the inner hysteresis-based current control (HCC) loop. The PMSG's rotor speed, ωm, is compared to the control loop's value. The reference rotor speed ωm and the outer speed are estimated by the MPPT method; the PI controller processes the speed error to obtain the reference T_e^* .

$$T_e^* = k_{ps}.[\ (\omega_{m*} - \omega_m) + \frac{1}{T_{is}}\int_0^t (\omega_{m*} - \omega_m)\, d\tau] \quad (10)$$

The integral time constant is T_{is}, and Kps is the proportional gain.
In the Laplace domain, after transforming Equation (18), we have

$$T_e^* = k_{ps}\left(\frac{1+pT_{is}}{pT_{is}}\right).(\omega_{m*} - \omega_m) \quad (11)$$

The reference torque T_e^* is then used to estimate the reference q-axis stator current Iq using Equation (T_e). To obtain a high torque-to-current ratio and avoid demagnetization for the surface type PMSG, the reference d-axis stator current ID is often equal to zero. The actual and reference three-phase stator currents are compared, and the resulting errors are then managed by an (HCC). The reference three-phase stator currents, *i*abc*, are calculated by applying inverse Park's transformation to the reference d-q axes stator currents. When the hysteresis band is appropriately selected, the MSC's switching frequency remains within its specified range [8].

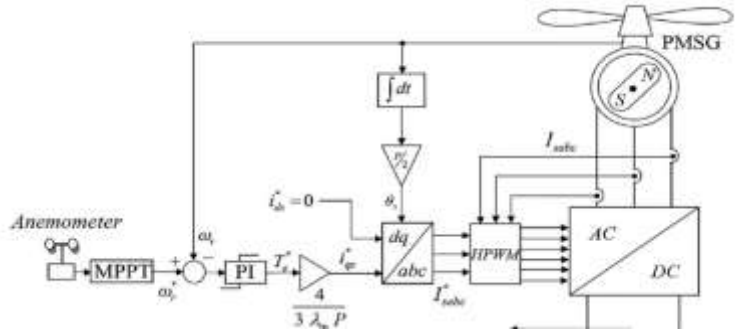

Fig 4. Machine side control [8]

E. Methodology and implementation of grid-side controllers

The structure of the wind farm is utilized in this investigation. It comprises a 60 KW generator with a PMSG according to an integrated DC bus. The PMSG is connected to the DC bus via a rectifier, while the DC bus is connected to the grid by a single DIAC inverter. The grid receives generated electricity from the grid-side inverter. , maintains a constant DC Bus voltage, and controls the amount of reactive and active (Pg & Qg) power delivered to the grid during the wind speed variation. It can regulate the grid power factor. Direct power control (DPC) regulates the grid link's (Pg&Qg) values in real-time.
Using loops, the d-q synchronous reference frame decouples also regulate the input (Pg&Qg). In Fig. 5, There is shown. The DC voltage controller compensates for the output filter's cross-coupling effect in the synchronously rotating reference frame by using the outside control loop [6].

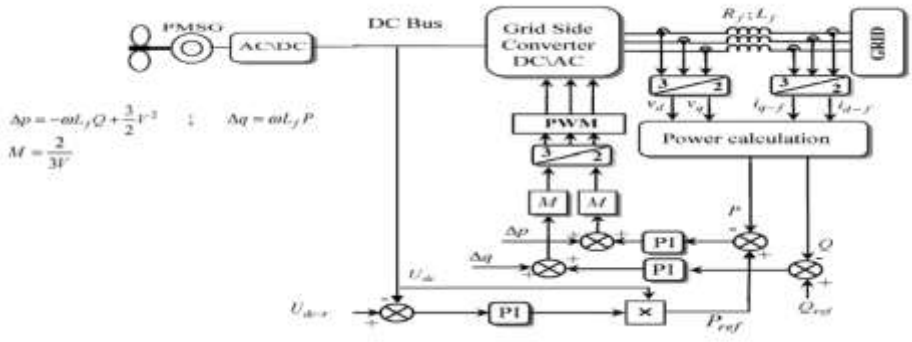

Fig 5. Grid side control [6]

III. CONTROL PHILOSOPHY

Due to their ability to correct the most accurate industrial processes, (PID) and (PI) controllers are widely used in manufacturing processes. For various control loops, controller blocks are selected as PI controllers. The designers' three main objectives for synthesizing an involved PI controller in a control loop are slight overshoot, good oscillation damping, and quick response. The ideal value of the rotor speed varies according to changes in wind speed. To get the rotor speed back to its optimal value, the PID controller lowers this finite error [28–30]. The design of the PI and PI^{α} controllers in several PMSG-based WECS control loops using the GWO, ARO, and RTH algorithms is covered in our research.

A. Grey Wolf Optimizer

The optimal fitness value for the GWO algorithm is believed to be alpha (α), beta (β), and gamma (γ) are, therefore, the second and third best. During a hunt, these three wolves are led to other packs. Grey wolves surround and disturb the prey until it stops after locating its prey. Therefore, to replicate the grey wolf's hunting style quantitatively, the first three best fitness values—alpha, beta, and gamma—should be kept. They can anticipate where their prey will be most likely to be found [31–35].

B. Artificial Rabbit Optimizer

ARO is

Derived from rabbits' natural survival methods. Real rabbits use ARO's foraging and hiding strategies, and the path their energy diminishes, and they switch between them [36-37].

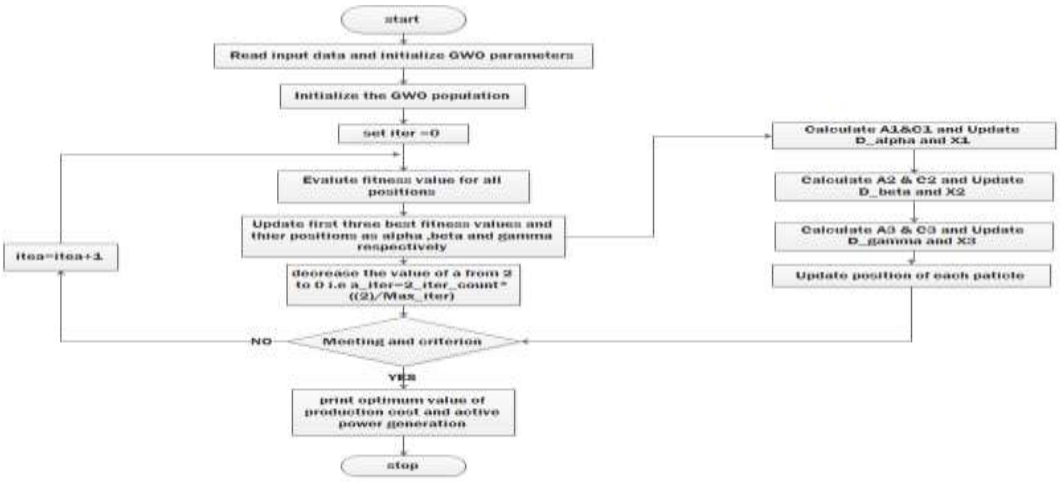

Fig 6. GWO flowchart

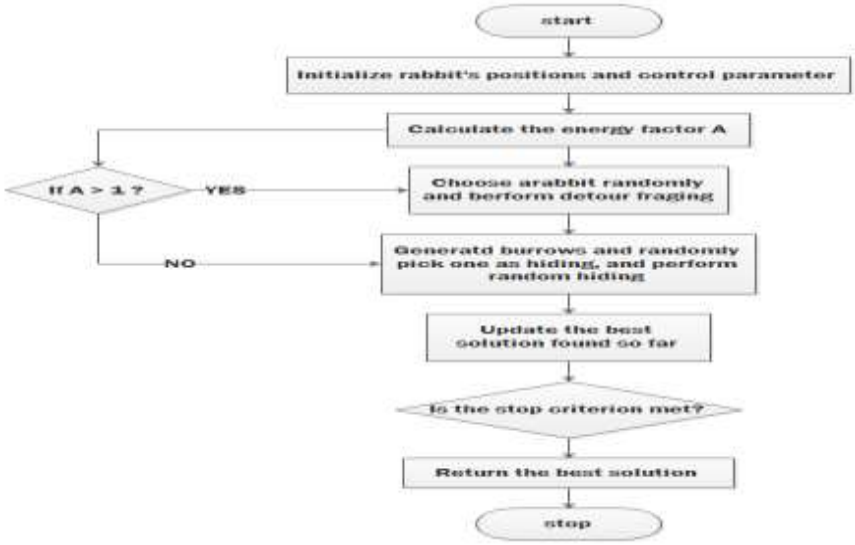

.

Fig. 7. ARO flowchart

C. Red-Tailed Hawk

The RTH concepts are better presented to understand the recommended RTH's characteristics and basics [38-43].

ALGORITHM 1: RTH PSEUDOCODE

```
Initialization: random generation within the search space.
While t<Tmax do
    High soaring stage: for i=1: Npop do
        Calculate Levy flight distribution Eq (2)
        Calculate the transition factor TF Eq (3)
        Update positions Eq (1)
    end
    Low soaring stage: for i=1: Npop do
        Calculate direction coordinates Eq (5)
        Update positions Eq (4)
    end
    Stooping and Swooping stage: for i=1: Npop do
        Calculate the acceleration and the gravity factors Eq (8)
        Calculate the step size Eq (7)
        Update positions Eq (6)
    end
end
```

Initially, the three algorithms were used and applied to 3 Benchmark functions: F_1 as a unimodal test function, F2 as a multimodal test function, and F3 as a low-dimensional multimodal test function; the table was made to compare the three methods regarding the finest solutions, mean, and standard deviation in Table 1.

Table 1. Comparison between ARO, RTH, and GWO in 3-benchmark function

FUN.	Index	ARO	RTH	GWO
$F_1(X) = \sum_{i=1}^{n} \lvert x_i \rvert + \prod_{i=1}^{n} \lvert x_i \rvert$	Best: Mean: Std:	3.5749e-72 5.8542e-83 5.8542e-83	0 0 0	9.1226e-26 0 0
$F_2(X) = \sum_{i=1}^{n} (x_i \, sin(\sqrt{\lvert x_i \rvert}))$	Best: Mean: Std:	-10990.138 -3351.7288 601.6778	-2944.6984 -1590.8041 318.6370	-1438.847 -6123.1 -408.44
$F_3(X) = [\frac{1}{500} + \sum_{J=1}^{25} \frac{1}{J+\sum_{i=1}^{2}(x_i - a_{ij})^6}]^{-1}$	Best: Mean: Std:	0.00030749 0.00030749 0	0.0003074 0.001606 0.0364	0.0010022 0.000337 0.000625

I then used all three optimizers to determine the kis and kps of my model. Each parameter's value is displayed using the Artificial Rabbit Optimizer in Table 2, the Grey Wolf Optimizer in Table 3, and the Red-Tailed Hawk in Table 4. The error signal contrast between the three techniques of control and without control is depicted in Figure 8.

Table 2. Kp's &Ki's Parameters Obtained by ARO

	KP1	KI1	KP2	KI2	KP3	KI3	KP4	KI4
ARO	258.8569	81.1215	0.264267	0.082824	0.300991	0.131486	0.32704	0.344607
	124.4041	76.8438	0.128923	0.165833	0.076117	0.174004	0.060829	0.442077
	259.191	73.3373	0.300419	0.056231	0.257883	0.41892	0.460395	0.249114
	197.9967	108.350	0.041635	0.330077	0.026153	0.278415	0.356013	0.243955
	100.9439	115.004	0.339266	0.126811	0.42159	0.146979	0.01343	0.046654

Table 3. Kp's & Ki's Parameters Obtained by GWO

	KP1	KI1	KP2	KI2	KP3	KI3	KP4	KI4
GWO	258.8569	81.1215	0.264267	0.082824	0.300991	0.131486	0.32704	0.344607
	124.4041	76.84388	0.128923	0.165833	0.076117	0.174004	0.060829	0.442077
	259.191	73.33738	0.300419	0.056231	0.257883	0.41892	0.460395	0.249114
	197.9967	108.3504	0.041635	0.330077	0.026153	0.278415	0.356013	0.243955
	100.9439	115.0041	0.339266	0.126811	0.42159	0.146979	0.01343	0.046654

Table 4. Kp's & Ki's Parameters Obtained by RTH

	KP1	KI1	KP2	KI2	KP3	KI3	KP4	KI4
RTH	189.3567	80.63495	0.254254	0.255386	0.408814	0.397416	0.322159	0.189305
	241.217	109.5336	0.376437	0.248361	0.432566	0.034014	0.484273	0.049378
	126.8685	149.8595	0.25676	0.193923	0.124926	0.182376	0.199529	0.46315
	228.434	70.69338	0.170094	0.163737	0.307482	0.295595	0.343962	0.083219
	125.8354	109.3175	0.360894	0.018513	0.088085	0.116218	0.357506	0.385293

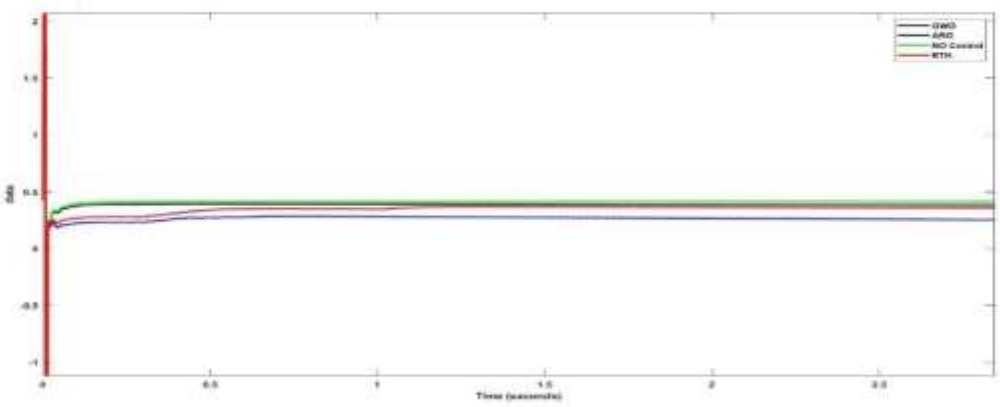

Fig 8. illustrates the contrast in the error signal between the three algorithms with and without PI control.

D. Fractional PI controller

Fractional-order calculus has been used to solve challenging mathematical and practical problems. It could help simulate any system that has memory and genetic characteristics. Fractional calculus is also utilized in automatic control to create more precise models enhance the performance of the control system and develop novel control strategies. When the GSC controller is adjusted to its ideal setting, unity power factor operation is guaranteed. The TSR MPPT approach based on FONPID An efficient FONPID controller has been proposed for MSC control to enhance the effectiveness of a well-established TSR MPPT approach. The TSR MPPT approach was chosen because of its effectiveness and fast reaction time. To get the generator speed to its ideal setting,
where the generator power reaches its maximum value for a given wind speed, managing the stator q-axis current achieves MPP effectively. A series of simulation results based on a step and turbulently altered wind profile show that the DC-link voltage has been modified to surpass the TSR MPPT approach based on PID and FOPID controllers in terms of minimizing the fitness function value and overshoot. In the meantime, the FONPID-based TSR MPPT approach minimizes the fitness function value, steady-state error, settling time, and overshoot more effectively than the PID-based MPPT approach [44-50].

Table 5. Kp's, Ki's&λ's Parameters Obtained by ARO

	KP1	KI1	λ1	KP2	KI2	λ2	KP3	KI3	λ3	KP4	KI4	λ4
ARO	0.374	0.1457	0.3477	0.2615	0.3988	0.1235	277.0713	142.6611	0.4809	0.0023	0.3875	0.4087
	0.253	0.1182	0.3177	0.2670	0.2588	0.3490	443.5036	415.6116	0.1589	0.2261	0.3761	0.0549
	0.252	0.2144	0.1195	0.2076	0.1703	0.1611	425.5118	257.3738	0.0268	0.1875	0.3875	0.0826

Table 6. Kp's, Ki's & λ's Parameters Obtained by GWO

	KP1	KI1	λ1	KP2	KI2	λ2	KP3	KI3	λ3	KP4	KI4	λ4
GWO	0.136	0.254	0.294	0.159	0.306	0.264	410.066	402.863	0.493	0.090	0.264	0.410
	0.3630	0.1450	0.1486	0.1924	0.1878	0.2003	211.6559	108.5853	0.3675	0.0253	0.2468	0.2048
	0.3882	0.2662	0.1344	0.1463	0.1764	0.2780	375.9949	155.2289	0.2143	0.4580	0.2949	0.2199

Table 7. Kp's, Ki's & λ's Parameters Obtained by RTH

	KP1	KI1	λ1	KP2	KI2	λ2	KP3	KI3	λ3	KP4	KI4	λ4
RTH	0.1218	0.1291	0.2549	0.3196	0.1853	0.3955	331.7783	474.9378	0.1193	0.4224	0.2259	0.0312
	0.1326	0.3145	0.1067	0.3993	0.1228	0.2177	232.8239	361.4570	0.2466	0.0117	0.0204	0.2020
	0.3934	0.2374	0.3929	0.1131	0.2656	0.3626	219.791	125.177	0.297	0.095	0.147	0.117

IV. RESULTS

After the PI controllers' parameters have been designed, the efficacy of the affected ones is assessed analytically using a comprehensive MATLAB/Simulink simulation model. It involves putting the optimal PI and PI^{α} controller parameter values into practice and examining how the PMSG-based WECS performs under various wind conditions. Figure. 9 displays the simulation findings' waveforms. The variation of the wind speed during a 3-second simulation in Figure a. ω_m of the PMSG's angular speed is illustrated in Figure b. These figures confirm the incredible precision of the control approaches under consideration. Figure c. displays the waveforms for the T_m of the (WT) and the T_e of the PMSG. The behavior of the PMSG T_e and the wind turbine's mechanical torque T_m is comparable. This is brought on by the control strategy's incredible accuracy and quick reactions.

Figure d. shows the waveforms of the instantaneous Pg provided to the AC grid vary in tandem with changes in wind speed. The DC link is represented by the voltage V_{dc} waveform in Figure E. Throughout the extensive range of fluctuations in wind velocity, the instantaneous values of voltage V_{dc} remain relatively constant. Figure F displays the waveforms of the stator current vector components I_d, I_q brought on by variations in wind speed. To maximize the torque per ampere ratio, the waveforms of the responses I_d, I_q, and wind speed fluctuations are comparable. Figure g. shows reactive power provided to the AC grid. This Figure shows that to meet the requirement of a unity power factor, the Qg is set to zero. Figure h. and Figure i illustrate grid current and voltage.

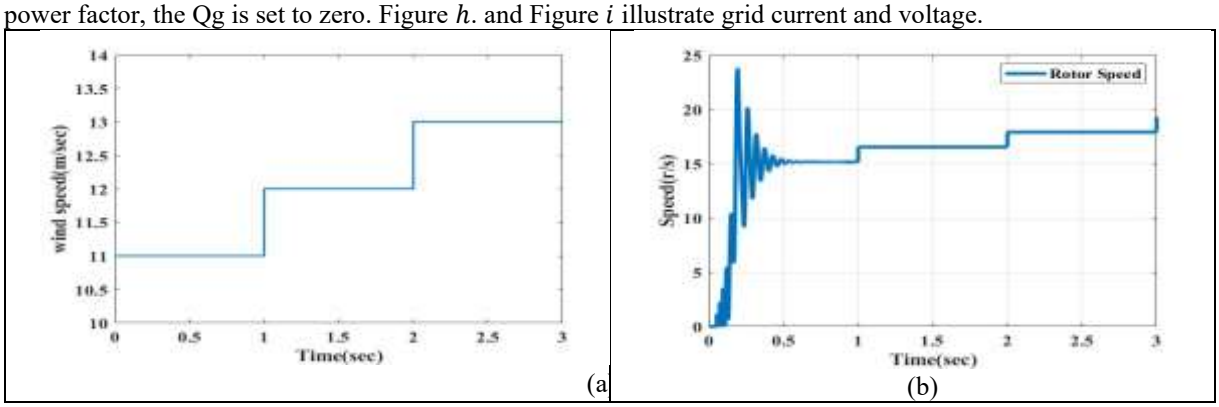

(a) (b)

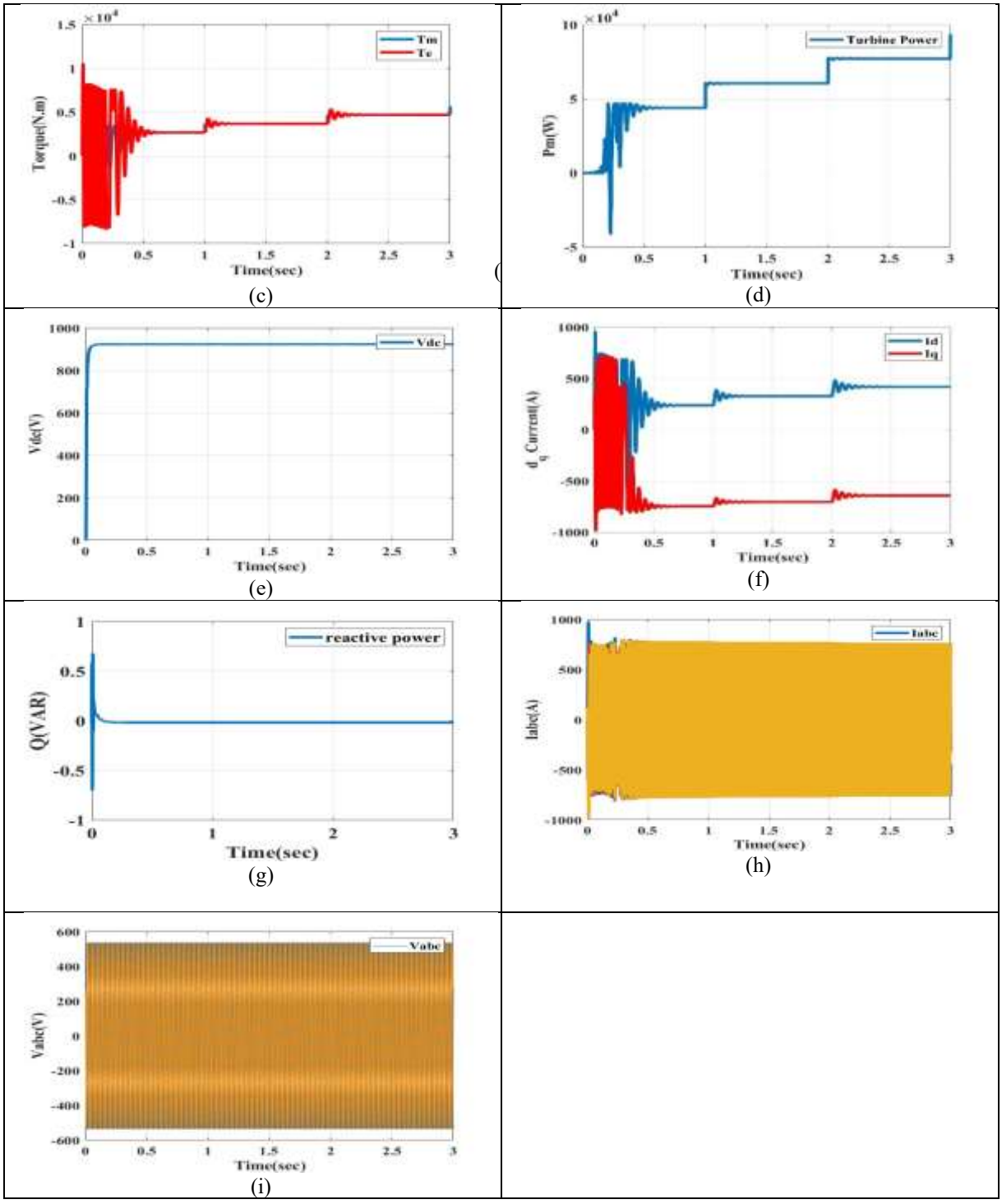

Fig 9. The PMSG-based (WECS) performs under different wind situations: (a) Rotor speed PMSG. (b)Torque mechanical and torque electrical, (c) Mechanical power. (d) dc-current. (e) dc-link voltage. (f) grid currents (g) grid voltages. (h) d-q axes PMSG stator currents

Table 8 compares the three optimizers at rated speed in Rise time, Max. Overshoot, Setting Time, and steady-state error using PI Controller and PI fractional controller. Figure 9 shows the difference between all three fractional PI controller algorithms.

Table 8. Wm step response at wind speed 12 m/s

	PI Fractional Controller	**PI Controller**
GWO	RiseTime: 0.1009 SettlingTime: 0.4588 Overshoot: 57.0863 Steady-state error: 0.0047	RiseTime: 0.1065 SettlingTime: 0.4586 Overshoot: 57.4166 Steady-state error: 0.0053
RTH	RiseTime: 0.1009 SettlingTime: 0.4590 Overshoot: 57.0359 Steady-state error: 0.0047	RiseTime: 0.1065 SettlingTime: 0.4595 Overshoot: 56.9410 Steady-state error: 0.0053
ARO	RiseTime: 0.1009 SettlingTime: 0.4588 Overshoot: 57.0834 Steady-state error: 0.0047	RiseTime: 0.1065 SettlingTime: 0.4607 Overshoot: 57.1309 Steady-state error: 0.0053

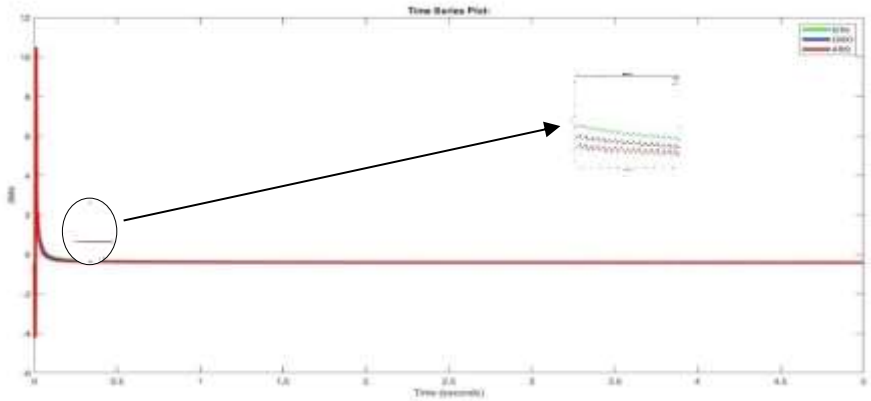

Fig 10. illustrates how the three algorithms with fractional PI control differ in terms of the error signal

V. CONCLUSION AND FUTURE WORK

Our research uses MATLAB Simulink to simulate the independent PMSG wind turbine system that feeds AC electricity to the utility grid. It also determines the control strategies, models, and designs of a 60 KW PMSG wind turbine. The model has a particular MSC control action that keeps the DC-link voltage constant by storing the active power surplus in the mechanical system moment of inertia of the generator and raising the rotor speed when the grid voltage decreases. The efficacy of the PI controller design is confirmed by the PMSG-based WECS's satisfactory operation with the suggested control structure under varied wind conditions. The MPPT method has been applied to GSC regulation. The DC link voltage is kept at the reference value, and the amount of Pg and Qg provided to the AC grid can be changed with the help of the GSC and MPPT. The generated reactive power is usually set to zero.

REFERENCES

[1] S.M. Saleh and A.Y. Hassan,''Sensorless based SVPWM-DTC of AFPMSM for electric vehicles". Sci Rep, Vol.12,pp.1-12,2022

[2] C.N Wang, W.C. Lin and X.K . Le, ''Modeling of a PMSG wind turbine with autonomous control''. *Mathematical Problems in Engineering*, Vol.2014, pp.1-9, May 2014

[3] M. Z bin Mohammad Suhaimi, A. A. Abd Samat , S. D Nor , N. A. Othman , I. H. Hamzah and Abdullah M. H . "Design and implementation of digital controller for DC-DC boost converter. *International Journal of Advanced Technology and Engineering Exploration*, Vol. *8 ,No.*(74), pp.12,2021

[4] M. Saber and S. Asmaa, "Evaluation of the Control Strategy Performance for Isolated Variable-Speed Wind Turbine Using Different Wind Speed Models at Different Load Cases under Balanced/Unbalanced Excitation", European Journal of Electrical Engineering, Vol.12 ,No.(4),pp.341-353,2019.

[5] A.Y. Hassan, A.M. Soliman, D. Ahmed and S. M. Saleh, "Wind cube optimum design for wind turbine using meta-heuristic algorithms". Alexandria Engineering Journal, Vol.61,No.(6), pp.4911-4929,2022.

[6] A. Soetedjo , A. Lomi ,and W. P. Mulayanto , "Modeling of the wind energy system with MPPT control". *In Proceedings of the 2011 International Conference on Electrical Engineering and Informatics*,pp.1-6,July 2011.

[7] E. Koutroulis ,and K. Kalaitzakis , " Design of a Maximum Power Tracking System for Wind-Energy-Conversion Applications", IEEE Transactions on Industrial Electronics, Vol.53, No. 2, pp.486-494,April 2006.

[8] A. Rolan , A. Luna , G. Vazquez, D. Aguilar and G. Azevedo, "Modeling of a variable speed wind turbine with a permanent magnet synchronous generator",*In 2009 IEEE international symposium on industrial electronics*,pp.734-739, July2009.

[9] T. Ackermann , Wind Power in Power Systems. New York: John Wiley &Sons, 2005.

[10] A. Y. Hassan, E. A. Ebrahim, S. M.Saleh and M. Elzalik. "Real-time advanced sensorless control of axial flux synchronous motor". International Journal of Power Electronics and Drive Systems (IJPEDS), Vol.15 ,No.3, pp.1358-1368,2024.

[11] M.A. Abdullah , A.H.M. Yatim , C.W. Tan and Saidur R , "A review of maximum power point tracking algorithms for wind energy systems". *Renewable and sustainable energy reviews*, Vol.16, No.5,pp.3220-3227,Mar.2012.

[12] M.A. Abdullah , A.H.M. Yatim an, C.W. Tan, "A study of maximum power point tracking algorithms for wind energy system". In: 2011 IEEE, first conference on clean energy and technology (CET),pp. 321-6, June2011.

[13] A. Y. Hassan, A. G. Rohieem and S. M. Saleh, "Direct Torque Control of Non-salient Pole AFPMSMs with SVPWM Inverter". International Journal of Power Electronics and Drive System (IJPEDS), Vol.13 ,No.4,pp.2014~2023,2022.

[14] J. Venkatesan, B. Manickam and S. Selvam , "MODELING and SIMULATION of PMSG-BASED WECS". *Advanced Materials Researc*h,Vol. 2014,pp.792-799,2017.

[15] X. Changliang , W. Zhiqiang , Sh. Tingna and S. Zhanfeng , "A Novel Cascaded Boost Chopper for the Wind Energy Conversion System Based on the Permanent Magnet Synchronous Generator" ,IEEE trans on energy conversion,Vol.28,No.3pp.512-522,June 2013.

[16] M. Abdelouahed , S. Abdellah, K. Mohamed , B. Omar and R. Abdelhadi , " BoosT Converter analysis to optimize variable speed PMSG Wind Generation System ", in Proc. 18th IEEE Int. Conf. pp.7-9 ,Mar. 2013.

[17] E. Muñoz-Palomeque , J. E. Sierra-García and M . Santos, "Wind turbine maximum power point tracking control based on unsupervised neural networks". *Journal of Computational Design and Engineering*, Vol. *10, No.*1,pp.108-121 , Dec.2022

[18] M. Yin , G . Li, M. Zhou and C. Zhao , "Modeling of the Wind Turbine with a Permanent Magnet Synchronous Generator for Integration". *IEEE*,Vol.1,pp.244-250.

[19] N. A. Mohamed , H. M. Hasanien , A. Alkuhayli , T. Akmaral , F. Jurado and A. O. Badr , " Hybrid Particle Swarm and Gravitational Search Algorithm-Based Optimal Fractional Order PID Control Scheme for Performance Enhancement of Offshor Wind Farms". ,Vol.2 ,*N*o.15, pp.11912.

[20] K. A. S. AbdElrazek, S. M. Saleh, A. Y. Hassan and K. H. Ibrahim. "White Shark based optimization of a Stand-alone PV System with Different Tracking Techniques"; 2023 24th International Middle East Power System Conference (MEPCON), Mansoura, Egypt, pp.1-8,2023.

[21] K. Roummani , K. Koussa , L. Saihi , F. Ferroudji , R. Maouedj and I. Yaichi , " Meta-Heuristics Optimization Based MPPT control of Wind Energy Conversion System with Permanent Magnet Synchronous Generator", 2023 Second International Conference on Energy Transition and Security (ICETS), Adrar, Algeria, pp. 1-6, 2023.

[22] P. Gajewski and K . Pieńkowski, "Control of a variable speed wind turbine system with PMSG generato"r. *Maszyny Elektryczne: zeszyty problemowe*,Vol.107 ,No.3,pp.75-80

[23] M. Baskar , V. Jamuna and S. D. Senthoor, " Simulation and Modeling of SVM based WECS with PMSG using Cuk Converter". Applied Mechanics and Materials,Vol.622,pp.163-172.

[24] M. F. Elmorshedy , S. M. Allam , A. I. Shobair and E. M . Rashad, "Voltage and frequency control of a stand-alone wind-energy conversion system based on PMSG". In 2015 4th International Conference on Electric Power and Energy Conversion Systems (EPECS) IEEE,pp.1-6,2015.

[25] S.M. Saleh and A. S. Farag, "Review Fixed-speed Wind Turbine Control Strategies for Direct Grid Connection", European Journal of Electrical Engineering ,Vol.1 ,No.23, pp.309-315,2019.

[26] B. Yang , T. Yu , H. Shu , X. Zhang , K. Qu and L. Jiang , "Democratic joint operations algorithm for optimal power extraction of PMSG based wind energy conversion system". *Energy Conversion and Management*, Vol.*159*,pp. 312-326, Jan 2018.

[27] N. H. Saad , A. A. El-Sattar and M. E. Marei , "Improved bacterial foraging optimization for grid connected wind energy conversion system based PMSG with matrix converter". *Ain Shams Engineering Journal*, Vol.*9,N*o.4 ,pp. 2183-2193, May.2017.

[28] S.M. Tripathi , A.N. Tiwari and D. Singh, "Optimum design of proportional-integral controllers in grid-integrated PMSG-based wind energy conversion system". *International Transactions on Electrical Energy Systems*, Vol.*26,N*o.5, pp.1006-1031 ,Augest2015.

[29] A. O'dwyer , "Handbook of PI and PID controller tuning rules" :World Scientific ;2009.

[30] J.C. Basilio and S. R. Matos , "Design of PI and PID controllers with transient performance specification". *IEEE Transactions on education*, Vol.*45,* No.4,pp. 364-370,Dec.2002.

[31] B. Kristiansson ,and B. Lennartson , "Robust tuning of PI and PID controllers: using derivative action despite sensor noise". *IEEE Control Systems Magazine*,Vol. *26,* No.1,pp. 55-69,2016.

[32] K. Teeparthi and D.V. Kumar, "Grey wolf optimization algorithm-based dynamic security constrained optimal power flow. *In 2016 National Power Systems Conference (NPSC*), Dec. 2016.

[33] M. H. Qais , H. M. Hasanien and S.A. Alghuwainem , " grey wolf optimizer for optimum parameters of multiple PI controllers of a grid-connected PMSG driven by variable speed wind turbine". *IEEE Access*,Vol. *6*,pp.44120-44128,2018.

[34] S. Mirjalili , S.M. Mirjalili and A . Lewis, "Grey wolf optimizer". *Advances in engineering software*, Vol.*69* ,pp. 46-61, Jan.2014.

[35] I.A. Zamfirache , R.E. Precup , R.C. Roman and E.M. Petriu, "Policy iteration reinforcement learning-based control using a grey Wolf optimizer algorithm". Inform.Sci. Vol.24,pp. 162–175,Nov. 2022.

[36] L. Wang , Q. Cao , Z. Zhang , S. Mirjalili and W. Zhao , "Artificial rabbits optimization: A new bio-inspired meta-heuristic algorithm for solving engineering optimization problems". *Engineering Applications of Artificial Intelligence*, Vol.11pp. 1-6, July2022.

[37] I. Boussaïd , J. Lepagnot and P. Siarry , "A survey on optimization metaheuristics". *Information sciences*,Vol. 7, pp.82-117,2023.

[38] S. Ferahtia , A. Houari , H. Rezk , A. Djerioui , M. Machmoum , S. Motahhir and A.A. Mourad , " Red-tailed hawk algorithm for numerical optimization and real-world problems". *Scientific Reports,Vol.* 13 ,No.1,pp.1-43,2023.

[39] M. M. Mousa, S. M. Saleh, M. M. Samy and S. Barakat. "Techno-Economic Analysis and Simulation of Electric Vehicle Charging Stations based on Green Energy System". 2023 24th International Middle East Power System Conference (MEPCON), Mansoura, Egypt, pp.1-6,2023.

[40] S.M. Saleh, A. S. Farag and G. M. El-Bayoumi. "Pitch Control Dynamic study of Isolated Wind Turbine based Self-Excited Induction Generator under Realistic Wind Speed Profiles". 2017 Nineteenth International Middle East Power Systems Conference (MEPCON), Menoufia University, Egypt, 19-21 December 2017.

[41] J. M. Ballam, " The use of soaring by the red-tailed Hawk (Buteo jamaicensis) ": Auk 101, 519–524 ;1984 .

[42] L. Day, The City Naturalist: "Red Tailed Hawk: in *The 79th Street Boat Basin Flora and Fauna Society;* 2007.

[43] R. L. Knight , D.E. Andersen , M.J. Bechard and N.V. Marr, "Geographic variation in nest-defence behaviour of the Red-tailed Hawk Buteo jamaicensis". *Ibis*,Vol.*131 ,No.*1, pp.22-26, Jan.1989 .

[44] D. Pathak , S. Bhati and P. Gaur , "Fractional-order nonlinear PID controller based maximum power extraction method for a direct-driven wind energy system". International Transactions on Electrical Energy Systems, Vol.30, No.12, e12641,2020.

[45] A. Bakry, M. Said and S. M. Saleh, "Proposed Design for Single Axis Photovoltaic Solar Tracker". MANSOURA ENGINEERING JOURNAL, (MEJ), Vol.45, No.2,pp. E1-E11,2020.

[46] R. Melício, Mendes VMF, Catal~ao JPS. " Fractional-order control and simulation of wind energy systems with PMSG/full-power convertertopology". Energy Convers Manage. Vol.51, No.(6),pp.1250-1258,2010.

[47] B. Yang, T. Yu, H. Shu, Y. Han, P. Cao and L. Jiang, " Adaptive fractional-order PID control of PMSG-based wind energy conversion system for MPPT using linear observers". Int Trans Electro Energy Syst. Vol.29, No.(1),pp.1-18,2019.

[48] I. Petráš, Fractional-order nonlinear controllers: design and implementation notes. Paper presented at: 2016 17th InternationalCarpathian Control Conference (ICCC),Vol.20; Tatranska Lomnica, Slovakia:pp.579-583, May 2016.

[49] A. Kumar, PJ. Gaidhane and V. Kumar, "A nonlinear fractional order PID controller applied to redundant robot manipulator". Paper presented at: 2017 6th International Conference on Computer Applications In Electrical Engineering-Recent Advances (CERA); October2017; Roorkee, India:527-532.

[50] H. Seraji, A new class of nonlinear PID controllers. IFAC Proc. Vol.30, no.20, pp.65-71.1997.